Development and Verification of Damage Prediction Method for 2D Plate Structures

Bor-Tsuen Wang, Huai-Chih Chang
Department of Mechanical Engineering
National Pingtung University of Science and Technology
wangbt@mail.npust.edu.tw, m9332028@mail.npust.edu.tw

ABSTRACT

This work adopts strain energy method as the damage detection index and combines the Lagrange-Interpolation method (LIM) as well as differential quadrature method (DQM) to develop the damage detection algorithm for 2-D structures. By performing either theoretical or experimental modal analysis on the structure, one can obtain the damaged and non-damaged structural mode shapes, that are the input to the prediction program. Therefore, the damage location can be detected. This work uses ANSYS software to construct both the damaged and non-damaged plate models and determine their mode shapes. The LIM is introduced to expand the measurement points and the DQM is applied to determine the derivatives of mode shapes, and so forth the damage index over the plate structure can also be expanded and beneficial to identify the damage location. Results show that the effectiveness of damage detection can be improved, especially for those experimental data limited. The employment of LIM can increase the accuracy of damage detection. The methodology can be applied to 1-D structures or even general 2-D structures.

Keywords: Lagrange-Interpolation Method (LIM). Differential Quadrature Method (DQM). Strain Energy Method (SEM).

1. INTRODUCTION

For a structure with damage, from the point of view of vibration the physical characteristics, such as natural frequencies, mode shapes and modal damping can be deviated from the normal or non-damaged structure. From the change of such physical insight, a non-destructive detection method can be developed to identify the damage, or even to predict the location and level of damage.

Chondros *et al.*[1] developed a theoretical model for the continuous defected beam and predicted the location of damages either on one side or both sides of simply supported beam. Their theory comes from Christides and Barrys. Xia and Hao[2] utilized the natural frequency data and calculated the probability density function of the input random signal as well as structural mass and stiffness matrices. From the change of the parameters before and after damaged, the damage location can be predicted. Cornwell *et al.*[3]used the derivatives of mode shape data to determine the strain energy for both 1-D beam and 2-D plate structures and can accurately predict the damage location. Shi *et al.*[4] also used strain energy method(SEM) as the damage index to successfully predict the energy change before and after damaged. They indicated that the index is related to system mass and stiffness matrices as well as structural mode shape and natural frequencies.

Teo *et al.*[5] applied differential quadrature method (DQM) to analyze be buckling of rectangular plate. DQM can be used to obtain any order of derivative or partial derivative of a function with the predefined variables and their corresponding function values. Tsao[6] applied the advantage of DQM in conjunction with SEM to damage detection for a 2-D plate. Although the detection is feasible, in practice the acquisition data points along the structure surface can be limited and resulted in inaccurate prediction.

This work adopts the structural mode shapes before and after damaged to predict the damage and its location for 2-D plate structure. ANSYS software is used to construct both normal and damaged plates. The line crack damage is simulated. The original mode shape data can be expanded with more data points by LIM, and the derivatives of mode shapes can then be calculated by DQM and used to obtain strain energy. Therefore, the damage index base on SEM can be determined and visualized to predict the damage location.

2. DAMAGE PREDICTION METHOD

This work develops a damage detection method. Figure 1 shows the flow chart for the procedures. First, ANSYS software is used to construct both normal and damaged plate models and obtain structural mode shapes before and after damaged. Only limited number of grid elements is used to simulate the practical experiments. Second, an expanded set of data points base on the original structural mode shapes is numerically generated by LIM. Third, the partial derivations of mode shapes that can be obtained by DQM are used to catenulate the strain energy. Finally, the damage index base on SEM can be determined and visualized to show the damage prediction results.

2.1 Lagrange-Interpolation method (LIM)

As mentioned, there are limited measurement points in performing practical modal testing on a structure. This work adopts LIM to numerically generate an expanded set of data points that are structural mode shapes in this paper.

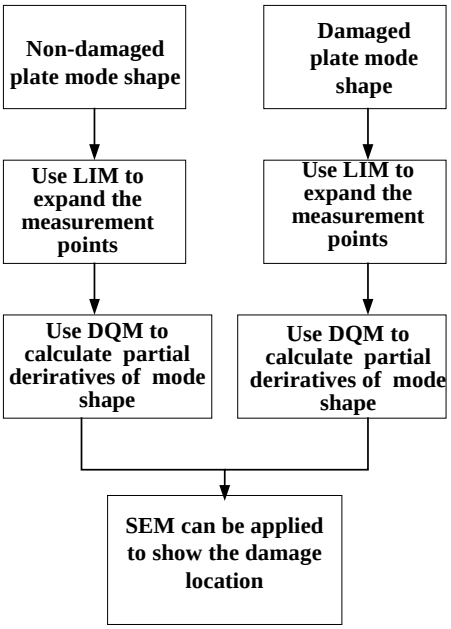

Figure 1. The flow chart for the prediction procedures

Considering the grid coordinates in a 2-D plate is (x_i, y_j) where $i = 1,2,...,N_x$ and $j = 1,2,...,N_y$. The corresponding mode shape at (x_i, y_j) is denoted as:

$$z_{ij} = z(x_i, y_j) \tag{1}$$

If the expanded set of data points is $(\bar{x}_r, \bar{y}_s)$ where $r = 1,2,...,\bar{N}_x$ and $s = 1,2,...,\bar{N}_y$, then the new mode shape values determined by LIM are：

$$\bar{z}_{rs} = \bar{z}(\bar{x}_r, \bar{y}_s) = \sum_{i=1}^{N_x}\sum_{j=1}^{N_y} z_{ij} F_i(\bar{x}_r) F_j(\bar{y}_s) \tag{2}$$

where

$$F_i(\bar{x}_r) = \frac{\prod_{k=1,k\neq r}^{N_x}(\bar{x}_r - x_k)}{\prod_{k=1,k\neq i}^{N_x}(x_i - x_k)} \tag{3}$$

$$F_j(\bar{y}_s) = \frac{\prod_{l=1,l\neq j}^{N_y}(\bar{y}_s - y_l)}{\prod_{l=1,l\neq j}^{N_y}(y_j - y_l)} \tag{4}$$

2.2 Differential Quadrature Method (DQM)

DQM[5] is an efficient and accurate numerical method and frequently used to solve for non-linear PDEs. The main future of DQM is that the partial derivatives of a function can numerically evaluated by multiplication of a weighting function. The calculation of the function derivatives is nothing more than the linear algebra.

If the function $z(x_i, y_j)$ where $i = 1,2,...,N_x$ and $j = 1,2,..,N_y$ are known, the partial derivatives of $z(x_i, y_j)$ at (x_i, y_j) can be expressed：

$$z_x^{(n)}(x_i, y_j) = \sum_{r=1}^{N_x} C_{ir}^{(n)} f(x_r, y_j);\ n = 1,2,...,N_x - 1 \tag{5}$$

$$z_y^{(m)}(x_i, y_j) = \sum_{s=1}^{N_y} \bar{C}_{js}^{(m)} f(x_i, y_s);\ m = 1,2,...,N_y - 1 \tag{6}$$

$$z_{xy}^{(n+m)}(x_i, y_j) = \sum_{r=1}^{N_x} C_{ir}^{(n)} \sum_{s=1}^{N_y} \bar{C}_{js}^{(m)} f(x_r, y_s)$$

$$i = 1,2,...N_x, \text{ and } j = 1,2,...,N_y \tag{7}$$

where $z_x^{(n)}(x_i, y_j)$ denotes the n^{th} partial derivatives of $z(x,y)$ with respect to x at (x_i, y_j); $z_y^{(m)}(x_i, y_j)$ denotes the m^{th} partial derivatives of $z(x,y)$ with respect to y at (x_i, y_j); $z_{xy}^{(n+m)}(x_i, y_j)$ denotes the n^{th} and m^{th} partial derivatives of $z(x,y)$ with respect to x and y partial, respectively, at (x_i, y_j); $C_{ir}^{(n)}$ and $\bar{C}_{js}^{(m)}$ are the weighting coefficients for the n^{th} and m^{th} partial derivatives of $z(x,y)$ with respect to x and y, respectively, and expressed as follows:

$$C_{ir}^{(n)} = n\left(C_{ii}^{(n-1)} C_{ir}^{(1)} - \frac{C_{ir}^{(n-1)}}{x_i - x_r}\right)$$

$$i, r = 1,2,...,N_x, r \neq i$$
$$n = 2,3,...,N_x - 1 \tag{8}$$

$$\bar{C}_{js}^{(m)} = m\left(\bar{C}_{jj}^{(m-1)} \bar{C}_{js}^{(1)} - \frac{\bar{C}_{js}^{(n-1)}}{y_j - y_s}\right)$$

$$j, s = 1,2,...,N_y, s \neq j$$
$$m = 2,3,...,N_y - 1 \tag{9}$$

where

$$C_{ii}^{(n)} = -\sum_{r=1,r\neq i}^{N_x} C_{ir}^{(n)}$$
$$i = 1,2,...,N_x$$
$$n = 1,2,...,N_x - 1 \tag{10}$$

$$\bar{C}_{jj}^{(m)} = -\sum_{s=1,s\neq j}^{N_y} \bar{C}_{js}^{(m)}$$
$$j = 1,2,...,N_y$$
$$m = 1,2,...,N_y - 1 \tag{11}$$

and

$$C_{ir}^{(1)} = \frac{M^{(1)}(x_i)}{(x_i - x_r)M^{(1)}(x_r)}$$
$$i, r = 1,2,...,N_x, r \neq i \tag{12}$$

$$\bar{C}_{js}^{(1)} = \frac{P^{(1)}(y_j)}{(y_j - y_s)}$$
$$j, s = 1,2,...,N_x, j \neq s \tag{13}$$

where

$$M^{(1)}(x_i)=\prod_{r=1,r\neq i}^{N_x}(x_i-x_r) \tag{14}$$

$$P^{(1)}(y_j)=\prod_{s=1,s\neq j}^{N_y}(y_j-y_s) \tag{15}$$

2.3 Strain Energy Method (SEM)

The strain energy for a plate structure can be shown as follows [4]:

$$U=\frac{D}{2}\int_0^{L_y}\int_0^{L_x}\left[(\frac{\partial^2 w}{\partial x^2})^2+(\frac{\partial^2 w}{\partial y^2})+2\nu(\frac{\partial^2 w}{\partial x^2})(\frac{\partial^2 w}{\partial y^2})+2(1-\nu)(\frac{\partial^2 w}{\partial x\partial y})^2\right]dxdy \tag{16}$$

where

$$D=\frac{Et^3}{12(1-\nu^2)} \tag{17}$$

in which D is the rigidity of the plate; L_x and L_y are the length and width of the plate; t is the plate thickness; E and ν are Young's Modulus and Poisson's ratio of the plate; $w=w(x,y)$ is the lateral displacement of the plate, for the k^{th} mode shape of the plate $\phi_k(x,y)$, the strain energy can be written:

$$U_k=\frac{D}{2}\int_0^{L_y}\int_0^{L_x}\left[(\frac{\partial^2 \phi_k}{\partial x^2})^2+(\frac{\partial^2 \phi_k}{\partial y^2})+2\nu(\frac{\partial^2 \phi_k}{\partial x^2})(\frac{\partial^2 \phi_k}{\partial y^2})+2(1-\nu)(\frac{\partial^2 \phi_k}{\partial x\partial y})^2\right]dxdy \tag{18}$$

If there are N_x and N_y equal grid points in both x and y directions, for the assumptions of uniform plate and equal grid space, the strain energy in the small block can be simplified as follows:

$$U_{ijk}=\frac{D_{ij}}{2}\left[(\frac{\partial^2 \phi_{ijk}}{\partial x^2})^2+(\frac{\partial^2 \phi_{ijk}}{\partial y^2})+2\nu(\frac{\partial^2 \phi_{ijk}}{\partial x^2})(\frac{\partial^2 \phi_{ijk}}{\partial y^2})+2(1-\nu)(\frac{\partial^2 \phi_{ijk}}{\partial x\partial y})^2\right]_{i=1,2,...N_x;\,j=1,2,...,N_y} \tag{19}$$

where

$$D_{ij}=\left[\frac{Et^3}{12(1-\upsilon^2)}\right]_{ij} \tag{20}$$

the strain energy for the k^{th} mode is：

$$U_k=\sum_{j=1}^{N_y}\sum_{i=1}^{N_x}U_{ijk} \tag{21}$$

The non-dimensional strain energy can be defined:

$$F_{ijk}=\frac{U_{ijk}}{U_k} \tag{22}$$

Corresponding to Equations (18) and (19), the damaged plate equations can be obtained for U_k^* and U_{ijk}^*, respectively, only ϕ_{ijk} to be substituted by ϕ_{ijk}^*. The super script * denotes the damaged plate, the non-dimensional strain energy for the damaged plate is shown:

$$F_{ijk}^*=\frac{U_{ijk}^*}{U_k^*} \tag{23}$$

Since the crack damage is small, the total strain energy before and after damaged remain constant, i.e.,

$$\sum_{j=1}^{N_y}\sum_{i=1}^{N_x}F_{ijk}=\sum_{j=1}^{N_y}\sum_{i=1}^{N_x}F_{ijk}^*=1 \tag{24}$$

and

$$U_k=U_k^* \tag{25}$$

Also, for a small region where is no damage, i.e., the strain energy is equal,

$$F_{ijk}=F_{ijk}^* \tag{26}$$

Redefine Equation (19)

$$U_{ijk}=\frac{1}{2}D_{ij}\times f_{ijk} \tag{27}$$

similarly,

$$U_{ijk}^*=\frac{1}{2}D_{ij}^*\times f_{ijk}^* \tag{28}$$

From Equations (23),(24),(27)

$$\frac{U_{ijk}}{U_k}=\frac{U_{ijk}^*}{U_k^*} \tag{29}$$

and from Equation(26)

$$D_{ij}\times f_{ijk}=D_{ij}^*\times f_{ijk}^* \tag{30}$$

One can obtain:

$$\frac{D_{ij}}{D_{ij}^*}=\frac{f_{ijk}^*}{f_{ijk}} \tag{31}$$

where

$$f_{ijk}=\frac{\int_{y_j}^{y_{j+1}}\int_{x_i}^{x_{i+1}}\left[(\frac{\partial^2 \phi_{ijk}}{\partial x^2})^2+(\frac{\partial^2 \phi_{ijk}}{\partial y^2})+2\nu(\frac{\partial^2 \phi_{ijk}}{\partial x^2})(\frac{\partial^2 \phi_{ijk}}{\partial y^2})+2(1-\nu)(\frac{\partial^2 \phi_{ijk}}{\partial x\partial y})^2\right]dxdy}{\int_0^{l_y}\int_0^{l_x}\left[(\frac{\partial^2 \phi_{ijk}}{\partial x^2})^2+(\frac{\partial^2 \phi_{ijk}}{\partial y^2})+2\nu(\frac{\partial^2 \phi_{ijk}}{\partial x^2})(\frac{\partial^2 \phi_{ijk}}{\partial y^2})+2(1-\nu)(\frac{\partial^2 \phi_{ijk}}{\partial x\partial y})^2\right]dxdy}$$

$$=\frac{\left[(\frac{\partial^2 \phi_{ijk}}{\partial x^2})^2+(\frac{\partial^2 \phi_{ijk}}{\partial y^2})+2\nu(\frac{\partial^2 \phi_{ijk}}{\partial x^2})(\frac{\partial^2 \phi_{ijk}}{\partial y^2})+2(1-\nu)(\frac{\partial^2 \phi_{ijk}}{\partial x\partial y})^2\right]_{i=1,2,3,...N_x;\,j=1,2,3,...,N_y}}{\sum_{j=1}^{N_y}\sum_{i=1}^{N_x}\left[(\frac{\partial^2 \phi_{ijk}}{\partial x^2})^2+(\frac{\partial^2 \phi_{ijk}}{\partial y^2})+2\nu(\frac{\partial^2 \phi_{ijk}}{\partial x^2})(\frac{\partial^2 \phi_{ijk}}{\partial y^2})+2(1-\nu)(\frac{\partial^2 \phi_{ijk}}{\partial x\partial y})^2\right]} \tag{32}$$

To account the effect of all modes, the damage index is defined:

$$\beta_{ij}=\frac{\sum_{k=1}^{m}f_{ijk}^*}{\sum_{k=1}^{m}f_{ijk}} \tag{33}$$

To normalize β_{ij}, the damage index is redefined:

$$Z_{ij}=\frac{\beta_{ij}-\overline{\beta}_{ij}}{\sigma_{ij,\beta}} \tag{34}$$

where, $\overline{\beta}_{ij}$ is the average of β_{ij} and $\sigma_{ij,\beta}$ is the standard deviation of β_{ij} as follows:

$$\overline{\beta}_{ij}=\frac{\sum_{j=1}^{N_y}\sum_{i=1}^{N_x}\beta_{ij}}{N_x\times N_y} \tag{35}$$

$$\sigma_{ij,\beta}=\sqrt{\frac{(N_x\times N_y)\left(\sum_{j=1}^{N_y}\sum_{i=1}^{N_x}\beta_{ij}^2\right)-\left(\sum_{j=1}^{N_y}\sum_{i=1}^{N_x}\beta_{ij}\right)}{(N_x\times N_y)(N_x\times N_y-1)}} \tag{36}$$

It is noted that Z_{ij} is the damage index base on the SEM and can be visualized to predict the damage location.

2.4 Sampling Point in DQM

In DQM, in order to obtain more accurate calculation of derivatives, the sampling points (x_i, y_j) are important. The grid points proposed by Shu and Xue[7] are as follows:

$$x_i = \frac{L_x}{2}\left(1-\cos\frac{(i-1)\pi}{N_x-1}\right)$$

$$i = 1,2,...,N_x \tag{37}$$

$$y_j = \frac{L_y}{2}\left(1-\cos\frac{(i-1)\pi}{N_y-1}\right)$$

$$j = 1,2,...,N_y \tag{38}$$

The non-equal spatial data points are implemented in the prediction program to ensure the accurate results.

3. MODAL ANALYSIS OF THE PLATE

This section will present the finite element model to simulate both the normal and damaged plate. Table 1 shows the plate specification. Four cases of damaged plates are considered as shown in Figure 2. ANSYS software is adopted to construct the plate model described as follows:

(1) Element type: The linear quadrilateral shell element (SHELL 63) with 4 nodes and 6DOFs is used.
(2) Mesh plan: As shown in Figure 3, there are 30 by 20 divisions in x and y directions. There are 600 elements in the models.
(3) Constraints: No displacement constructs is prescribed for the free-free plate. There is also no force applied for modal analysis.

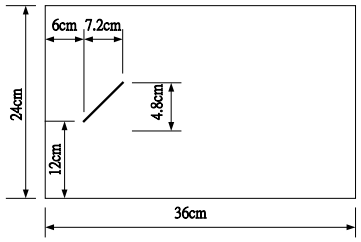

(a) Case A

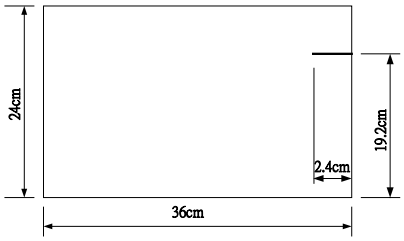

(b) Case B (One Crack)

Figure 2. Four cases of damaged plates

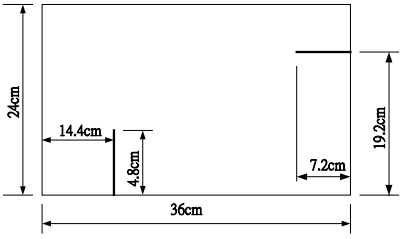

(c) Case C (Two Cracks)

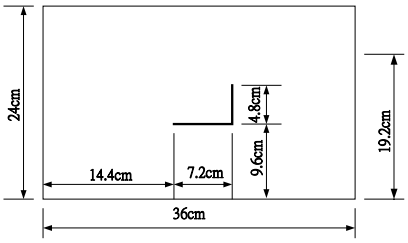

(d) Case D (Crack in the middle)

Figure 2. Four cases of damaged plates

Table 1. Plate specification

Material Properties	2D plate
Young's Modulus E	207×10^9 **N/m** ^{2}
Poisson's Ratio ν	**0.3**
Density ρ	**7870kg/m** ^{3}
Length L_x	**0.36m**
Width L_y	**0.24m**
Thickness t	**0.002m**

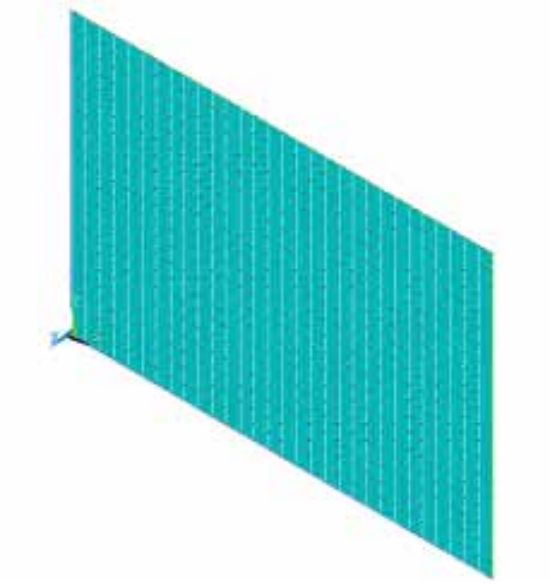

Figure 2. Finite element model from ANSYS software

To simulate the line crack damage in plate, the nodal points in lines are splitter and rearranged the connectivity of nodes ranged accordingly. The first eight flexible modes are considered and input to the damage prediction program.

4. RESULTS AND DISCUSSIONS

4.1 Effect of LIM

This paper introduces LIM to expand the mode shape data points due to experimental limitation. However, only simulation data from FEA is studied.

Figure 4 shows the damage prediction results for Case A, when (N_x, N_y)=(31,21), the grid points are sufficient enough to provide a very good damage prediction.

For only a few points being measured, i.e., (N_x, N_y)=(6,6), Figure 5 shows the prediction results for different $\overline{N}_x$ and $\overline{N}_y$. Discussions are as follows:

(1) In Figure 5(a), (N_x, N_y)=(6,6) and $(\overline{N}_x, \overline{N}_y)$=(6,6), i.e., no LIM is applied. Although the prediction is good, the specific region in not clears enough.

(2) Figure 5(b) and Figure 5(c) shows the prediction results for $(\overline{N}_x, \overline{N}_y)$=(12,12) and $(\overline{N}_x, \overline{N}_y)$=(18,18), respectively. One can observe that the damage zone can be more clearly shown.

(3) In comparison to Figure 4, the prediction results may not be good enough. However, it should be noted that there are only 6 data points in both x-direction and y-direction.

To further show the advantage of LIM, Figure 6 shows the prediction results of Case A for (N_x, N_y)=(16,11). Figure 6(a) is for no LIM applied, while Figure 6(b) is for the adoption of LIM with $(\overline{N}_x, \overline{N}_y)$=(21,16). One can see that the prediction of Figure 6(b) is better than Figure 6(a) and is similar to Figure 4. This clearly indicates that the employment of LIM to expand the data set reveals a great advantage for few data points.

Table 2 shows the prediction results for the other cases, when (N_x, N_y)=(16,11). $(\overline{N}_x, \overline{N}_y)$=(16,11) is for no LIM, and $(\overline{N}_x, \overline{N}_y)$= (31,21) is applied by LIM. Some observations are summarized as follows:

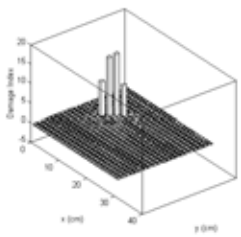

Figure 4. Prediction results for Case A, (N_x, N_y)=(31,21)

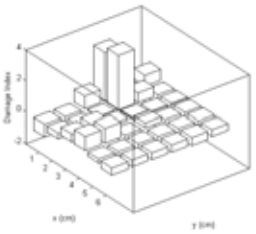

(a) $(\overline{N}_x, \overline{N}_y)$=(6,6)

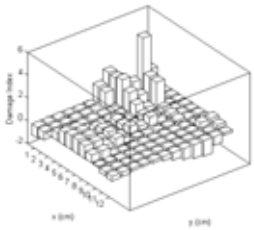

(b) $(\overline{N}_x, \overline{N}_y)$=(12,12)

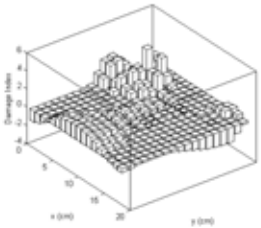

(c) $(\overline{N}_x, \overline{N}_y)$=(18,18)

Figure 5. Prediction results for Case A, (N_x, N_y)=(6,6)

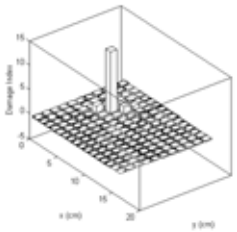

(a) $(\overline{N}_x, \overline{N}_y)$=(16,11)

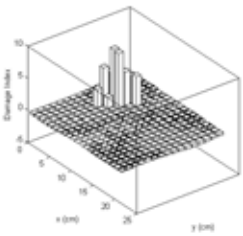

(b) $(\overline{N}_x, \overline{N}_y)$=(21,16)

Figure 6. Prediction results for Case A (N_x, N_y)=(16,11)

(1) The adoption of LIM to expand mode shape data points provides a better damage detection, in terms of revealing the damage zone more clearly.
(2) In case of few data points being obtained in experiments, the LIM can improve the deficiency of spatial resolution, and so forth provide a specific zone of damage prediction.

4.2 Experimental Validation

The experimental results from Tsao[7] are studied here. The same plate specification is as shown in Table 1. The damaged plate is similar to Case B except the location at one sixth of the plate. In experimental testing, there are only 36 measurement points, i.e., (N_x, N_y)=(6,6). Figure 7(a) is the prediction results for no LIM. One can see the false peak occurs at the corner. The damage detection is failed. However, with the trial of different $\overline{N}_x$ and $\overline{N}_y$ in Figure 7(b)-7(e), the damage location can be clearly identified. For $\overline{N}_x$ and $\overline{N}_y$ larger than 15, the perditions become failed. We may conclude that with the reasonable expansion of data points by LIM, the damage detection can be greatly improved.

Table 2.Prediction results for different case (N_x, N_y)= (16,11)

Case	$(\overline{N}_x, \overline{N}_y)$= (16,11)	$(\overline{N}_x, \overline{N}_y)$= (31,21)
B	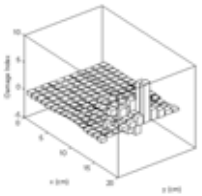	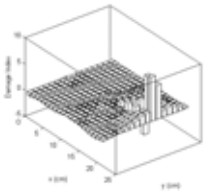
C	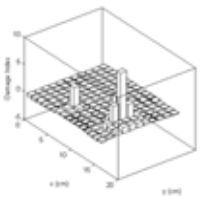	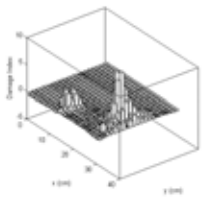
D	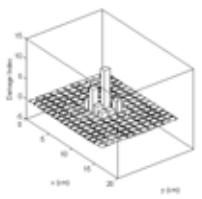	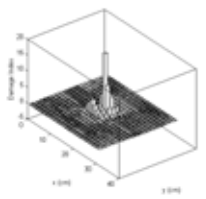

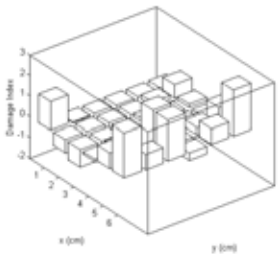

(a) $(\overline{N}_x, \overline{N}_y)$= (6,6)

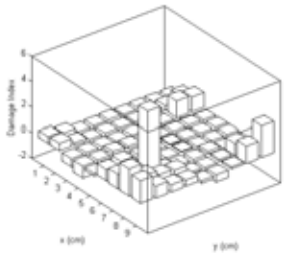

(b) $(\overline{N}_x, \overline{N}_y)$= (9,9)

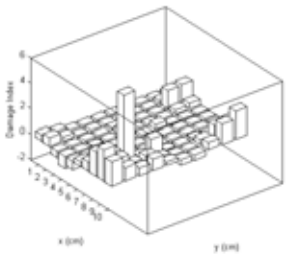

(c) $(\overline{N}_x, \overline{N}_y)$= (11,11)

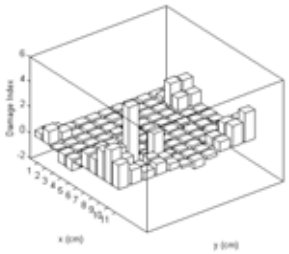

(d) $(\overline{N}_x, \overline{N}_y)$= (12,12)

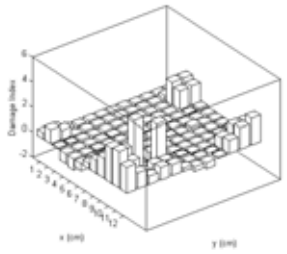

(e) $(\overline{N}_x, \overline{N}_y)$= (15,15)

Figure 7. Prediction results experimental data, (N_x, N_y)=(6,6)

5. CONCLUSIONS

This paper presents to include the LIM into the damage prediction algorithm in conjunctions with the DQM and SEM. The efficiency of using SEM to damage detection has been shown. In particular, the benefit of LIM to expand mode shape data points can be validated. An actual experimental result is also demonstrated that with the adoption of LIM the effectiveness of damage detention has been greatly improved. The developed methodology can be beneficial for vibration base damage detection method, especially for those limited measurement data points in practical experiments.

6. REFERENCES

[1] Chondros, T. G., Dimarogonas, A. D. and Yao, J., 1998, "A Continuous Cracked Beam Vibration Theory," *Journal of Sound and Vibration*, Vol. 215, No.1, pp.17-34.

[2] Xia, Y., and Hao, H., 2000, "Measurement Selection for Vibration-Based Structural Damage Identification," *Journal of Sound and Vibration*, Vol. 236, No.1, pp. 89-104.

[3] Cornwell, P., Doebling, S. W., and Farrar, C. R., 1999, "Application of the Strain Energy Damage Detection Method to Plate-Like Structures," *Journal of Sound and Vibration*, Vol. 224, No.2, pp. 359-374.

[4] Shi, Z. Y., Law, S. S., and Zhang, L. M., 1998, " Structural Damage Localization from Modal Strain Energy Change," Journal of Sound and Vibration, Vol.218, No.5, pp. 825-844.

[5] Teo, T. M., and Liew, K. M., 1999, "A Differential Quadrature Procedure for Three-Dimensional Buckling Analysis of Rectangular Plates," Journal of Solid and Structures, Vol. 36, pp.1149-1168.

[6] Wun-Chang Tsao, 2001, *Evaluation of Vibration Based Method for Structural Nondestructive Inspection*, National Pingtung University of Science and Technology. Pingtung, Tanwan. (In Chinese)

[7] Shu, C., and H. Xue, 1999,"Solution of Helmholtz Equation by Differential Quadrature Method," *Computer Method in Applied Mechanics Engineering*, Vol. 175, pp. 203-212.

二維平板結構之破壞預測發展與驗證

王栢村[1]　張懷智[2]

[1]國立屏東科技大學機械工程系研究所教授

[2]國立屏東科技大學機械工程系研究所研究生

wangbt@mail.npust.edu.tw, m9332028@mail.npust.edu.tw

摘要

本文主要利用應變能法(Strain Energy Method)為破壞檢測指標，結合 Lagrange-Interpolation 法(LIM)與微分值積法(Differential Quadrature Method, DQM)建立二維平板結構破壞預測程式。在進行理論與實驗的模態分析後，可獲得結構破壞或非破壞時的模態振型，並將此模態振型的資訊由程式運算，進而預測破壞發生的位置。本文利用有限元素軟體 ANSYS 建構破壞與非破壞的二維平板模型，可得到模態振型的資訊，經由 LIM 擴充其量測的點數，並由 DQM 求得振型的微分結果，可以有效的鑑定破壞的位置。結果顯示出此預測流程的方法可以有效的改進預測破壞檢測的指標，特別對量測點數不足之實驗數據，可明顯改善預測結果，因此利用 LIM 可以增加結構破壞檢測的正確性，未來此也方法可以應用在一維的結構或者是一般化二維平面結構的破壞預測。

關鍵字：Lagrange-Interpolation 法，微分值積法，應變能法